Alexandria Engineering Journal (2023) 65, 749–760

HOSTED BY

Alexandria University

Alexandria Engineering Journal

www.elsevier.com/locate/aej
www.sciencedirect.com

ORIGINAL ARTICLE

Power management optimization of electric vehicles for grid frequency regulation: Comparative study ☆

Mohamed Y. Metwly [a,*], Mohamed Ahmed [b], Mostafa S. Hamad [c], Ayman S. Abdel-Khalik [d], Eman Hamdan [e], Noha A. Elmalhy [d]

[a] *Smart -CI Center, Faculty of Engineering, Alexandria University, 21544 Alexandria, Egypt*
[b] *Engineering Mathematics and Physics Department, Faculty of Engineering, Alexandria University, 21544 Alexandria, Egypt*
[c] *Electrical and Control Engineering Department, Arab Academy for Science, Technology and Maritime Transport, Alexandria 1029, Egypt*
[d] *Electrical Engineering Department, Faculty of Engineering, Alexandria University, Alexandria 21544, Egypt*
[e] *Marine Engineering Technology Department, Arab Academy for Science, Technology and Maritime Transport, Alexandria 1029, Egypt*

Received 9 August 2022; revised 27 September 2022; accepted 10 October 2022
Available online 26 October 2022

KEYWORDS

Secondary frequency regulation (SFR);
Electric vehicles (EVs);
Multi-objective optimization;
Contingency cases;
Vehicle-to-grid (V2G)

Abstract Electric vehicles (EVs) have shown promise in providing ancillary services, e.g., frequency regulation. This is mainly due to their capacities and fast response. On the contrary, the rapid integration of EVs in the grid poses challenges, such as frequency and voltage stability. In order to mitigate the above-mentioned issues, several dispatching strategies have been introduced in the recent literature to optimize the charging/discharging rates of EVs. In this paper, a comparative study of power management strategies for secondary frequency regulation (SFR) employing a fleet of EVs is presented. A hierarchical control scheme is employed to compare two cases, namely control at the charging station (CS) level and novel control at the EVs level. Under both cases, a multi-objective optimization approach is utilized to define the optimal charging and discharging rates of EVs using a pattern search algorithm. Furthermore, the performance of the two models is experimented under contingency cases, a notable contribution of this study. Finally, simulations are carried out using OPAL-RT real time simulator to validate the performance of the two models based on real-time traces obtained from Pennsylvania, New Jersey, and Maryland (PJM) interconnection and California independent system operator (CAISO). To further validate the proposed model, a comparison with a mixed-integer linear programming (MILP) based model is presented.

* Corresponding author.
E-mail addresses: m.metwly@smartci.alexu.edu.eg (M.Y. Metwly), mohamed.abuyehia@alexu.edu.eg (M. Ahmed), mostafa.hamad@staff.aast.edu (M.S. Hamad), ayman.abdel-khalik@alexu.edu.eg (A.S. Abdel-Khalik), eman_youssef@aast.edu (E. Hamdan), noha.elmalhy@alexu.edu.eg (N.A. Elmalhy).

☆ This work was submitted on 4- August- 2022 and achieved by the financial support of ITIDAs ITAC collaborative funded project under the category type of advanced research projects (ARP) and Grant No ARP2020.R29.7.
Peer review under responsibility of Faculty of Engineering, Alexandria University.

https://doi.org/10.1016/j.aej.2022.10.030
1110-0168

Nomenclature

AG_i	i^{th} Aggregator
CS_{ij}	j^{th} Charging station of the i^{th} Aggregator
$C_{ij}^{sch}(T)$	Charging rate of the EVs at the j^{th} CS of the i^{th} AG at time interval T
$C_{ijk}^{sch}(T)$	Charging rate of the k^{th} EV at the j^{th} CS of the i^{th} AG at time interval T
C_{max}	Charging rate maximum limit
C_{min}	Charging rate minimum limit
$\mathscr{C}^{up}(T)$	Regulation up cost at time interval T
$\mathscr{C}^{down}(T)$	Regulation down cost at time interval T
$D_{ij}^{sch}(T)$	Discharging rate of the EVs at the j^{th} CS of the i^{th} AG at time interval T
$D_{ijk}^{sch}(T)$	Discharging rate of the k^{th} EV at the j^{th} CS of the i^{th} AG at time interval T
D_{max}	Discharging rate maximum limit
D_{min}	Discharging rate minimum limit
E_{ijk}^{rated}	Rated energy capacity of the k^{th} EV
EV_{ijk}	k^{th} Electric vehicle of the j^{th} Charging station of the i^{th} Aggregator
K	Number of EVs
M	Number of AGs
N	Number of CSs
$\mathscr{P}_i^{up}(T)$	Frequency regulation up capacity of the i^{th} AG at time interval T
$\mathscr{P}_i^{down}(T)$	Frequency regulation down capacity of the i^{th} AG at time interval T
$\mathscr{P}_{ij}^{up}(T)$	Frequency regulation up capacity of the j^{th} CS at time interval T
$\mathscr{P}_{ij}^{down}(T)$	Frequency regulation down capacity of the j^{th} CS at time interval T
$\mathscr{P}_{ijk}^{up}(T)$	Frequency regulation up capacity of the k^{th} EV at time interval T
$\mathscr{P}_{ijk}^{down}(T)$	Frequency regulation down capacity of the k^{th} EV at time interval T
$\mathscr{P}^{tot}(T)$	Total frequency regulation capacity at time interval T
SoC	State of charge
$SoC_{ijk}^{ini}(T)$	Initial state of charge of the k^{th} EV at time interval T
$SoC_{ijk}^{fin}(T)$	Final state of charge of the k^{th} EV at time interval T
SoC_{max}	State of charge maximum limit
SoC_{min}	State of charge minimum limit

1. Introduction

Due to the growing reliance on renewable energy sources (RES), frequency regulation mechanism has become a necessity to maintain supply and demand balance in smart grid (SG) [1]. Power fluctuations of RES such as wind turbines result in deviations in the grid's frequency, which, therefore, yield undesirable disturbances, e.g., brownouts, blackouts, and voltage fluctuations [2]. Thermal generators have been conventionally utilized to support the grid's frequency at the supply side; however, they cannot instantaneously eliminate the frequency deviations because of their limited ramp rate [3]. On the other hand, several agents can provide frequency regulation at the demand side such as commercial buildings and energy storage devices. Amongst demand-side agents, electric vehicles (EVs) have been seen as the most reliable agent to adjust the power balance between generation and consumption in real-time [4].

With the increasing EV market penetration, an EV aggregator can manage a large number of EVs to provide considerable regulation capacity. Automotive market analysis shows that the global market share of electric vehicles (EVs) will be about 30 % by 2030 [5]. According to the analysis presented in [5], Norway, Iceland, Netherland, and Sweden own the largest EVs market share. Despite the fact that EVs can offer effective frequency support, the growing reliance on electricity and stochastic charging/discharging performance constitute the main challenges of EVs participating in secondary frequency support. Thus, coordinated scheduling of EVs has been the topic of a significant body of literature [6]. Moreover, vehicle-to-grid (V2G) concept to allow bidirectional power flow between the grid and EVs has been introduced. Under V2G operation, the power can flow from the grid to the EV batteries under charging mode. Besides, the aggregated power can be delivered back to the grid. As a result, several ancillary services can be provided by EVs including spinning reserve, voltage stability, energy storage, and frequency regulation [7].

Several dispatching strategies employing either centralized or distributed schemes have been proposed in the literature highlighting the effective use of EVs for secondary frequency regulation [6,8]. In centralized mode, an aggregator controls a fleet of EVs, which are located at the charging station. Nevertheless, the EVs are located in public areas and controlled by the grid operator in distributed mode. Moreover, the hierarchical approach employs intermediate aggregation layers and coordinates the control signal between the aggregators and EVs to increase the system flexibility and scalability. As an illustrative example, a hierarchical control scheme of EVs for secondary frequency regulation (SFR) has been elaborated in [4]. The regulation signals are estimated at the physical layer, which comprises a substation unit, aggregators, and charging stations. While these regulation signals are segregated between the physical entities at the control layer. Eventually, the charging and discharging behaviors are optimized based on mixed-integer linear programming (MILP). Whereas, a distributed power control system based on the bidirectional V2G concept has been introduced in [9]. In order to estimate the regulation capacities, an energy supervision model has employed a day-ahead EV charging/discharging schedule. A nonlinear programming (NLP) optimization model is used to decrease the charging cost while concurrently reducing battery degradation. Moreover, a comprehensive analysis of SFR techniques using EVs has been conducted in [10,11], with further classification by the main aspect: frequency-aware and economic-aware. The former aims at maintaining the frequency at its nominal

value, e.g., 50 Hz and 60 Hz. Whereas the latter sheds light on the economical profits of EVs participating in frequency regulation. The effectiveness of using a fleet of EVs for secondary frequency support has been verified [12,13]. In [13], Yao *et al.* discussed how the independent system operator (ISO) in the U.S uses EVs to support the grid' frequency by changing the real-time charging/discharging behaviors with respect to an automatic generation control (AGC) signal. Furthermore, a novel controller has been recently presented to cluster the EVs with diverse state-of-charge (SoC) and average daily travel [14]. In that case, a multi-objective optimization model based on the Particle Swarm algorithm is applied to minimize the grid frequency imbalances, while concurrently accommodating the EVs' power needs. In [15], Latifi *et al.* proposed a novel control technique of EVs for frequency regulation services considering an active and reactive power compensation. This is beneficial not only to the car owners but also to the grid operator as it improves the grid security by supplying reactive power, which yields an enhanced voltage profile. In addition, Neofytou *et al.* investigated the feasibility of EVs for distributed frequency support in an isolated grid of Cyprus Island [16]. This study showed the benefits of using the aggregated power from EV batteries to the grid through V2G operation taking into consideration the user preferences.

In addition to the above-mentioned frequency-aware dispatching strategies, several economic-aware-based strategies have been proposed in the recent literature to encourage car owners to participate in frequency regulation services [3,7,12,17]. In [12], Han *et al.* presented a feasibility study of frequency regulation based on V2G operation, focusing on the economical earnings of the EV car owners. Not only EV' users but also grid operators can get revenues from the utilization of EVs in ancillary services. Minimizing the frequency fluctuation risen from the intermittency of renewable energy sources boosts the earnings of the grid operators; while decreasing the grid investments [10]. Latterly, a model predictive control (MPC) for an EV aggregator has been introduced in [3]. It maximizes the capacity payment for EV aggregators considering the regulation capacity prices. Based on the improved prediction model, capacity payment is increased by 4.3 % when compared to simple prediction one.

It can be noted that the topic of EVs participating in frequency regulation has gained the attention of researchers worldwide. Several optimization models have been applied considering various objectives, namely, MILP [4,7], NLP [9], and stochastic MILP [17]. For instance, the efficacy of using a fleet of EVs for secondary frequency support has been proved using a multi-objective primal problem (Mo-PP) [18]. The interior point method was used to solve the set of decomposed subproblems. Recently, An efficient state-space model has been presented to estimate the EVs regulation capacities and state transitions based on the Markov transition matrix [20]. It accurately achieves the real-time control of aggregated EVs with low computational workloads; albeit, at low pressure on real-time communications. An improved state-space model that considers the EV owners' preferences and the modeling error has been presented in [2]. This model - besides estimating the frequency regulation capacity - achieves the frequency regulation taking into consideration the progressive state recovery.

To summarize the aspects of the previous mentioned strategies, Table 1 reveals the broad comparison of these dispatching strategies considering system architecture, bidirectional V2G, maximum revenues, optimization algorithm, minimum battery degradation, time scheduled, and main purpose.

Contingencies in the power distribution network are likely to happen. To the best of the authors' knowledge, almost all publications in the area of EVs participating in the grid ancillary services have concentrated on frequency regulation strategies and control design. However, the assessment of a dispatching strategy under contingency conditions has not been presented thus far. The integration of fleet of EVs into the grid poses challenges, particularly at the distribution network level [21,22]. For instance, the EV charging station load considerably affects the voltage stability of the distribution network and yields higher peak load and lower reserve margins [23]. The rapid EV integration into the distribution network can be considered as an extra load at the demand side either with or without the inclusion of the power electronic converter [24]. This paper investigates the second approach excluding the power electronic converter. To emulate the contingency cases, several charging stations (CSs) are successively removed, while evaluating the proposed scheme to meet the regulation signal at each case.

According to the afore-mentioned investigation of dispatching strategies, it is clear that EVs constitute the optimal solution for secondary frequency support in the smart grid (at demand side). Therefore, it is challenging to optimize the charging/discharging performance of the EVs to instantaneously maintain the balance between the demand and supply sides, while providing the customer charging demand. In the recent literature, hierarchical control schemes have been introduced increasing the scalability and flexibility of the system. These power control schemes leverage the utilization of EVs for secondary frequency support and further underpin the bidirectional V2G concept. Another critical issue is the economical profits for both EV owners and grid operators. Minimum frequency deviations, optimal dispatch of the regulation signal, minimum battery degradation, and maximum revenues are among the proposed objectives. However, a system satisfying these objectives under contingency conditions, i.e., the loss of one or more charging stations, has not been conceived so far.

This paper presents a comparative study of the system performance at two different control layers, i.e., control of each EV charging/discharging behavior (Case 1) and control of a set of EVs in a charging station (Case 2). Thus, the minimum frequency imbalance is achieved, while considering the EV owners' preferences. The main contributions are summarized as follows:

- A reliable and scalable hierarchical control scheme is designed at two different layers to highlight the benefits of using EVs for SFR.
- Two cases are simulated and compared from efficiency and complexity perspectives.
- The charging/discharging behaviors of EVs are optimized formulating a multi-objective optimization problem based on the efficient pattern search algorithm.
- Simulations are carried out using Hardware-in-the-Loop via the OPAL-RT (real time simulator), shedding light on the comparison of the novel control model at the EVs and the conventional one at the CSs which are further com-

Table 1 Comparison of power control strategies for frequency regulation using EVs.

Ref.	System architecture	Max. revenues	Optimization/ Algorithm	Minimum Battery degradation	Time scheduled	Main purpose
[3]	centralized	Yes	MILP	No	Real-time	Economic-aware
	This paper proposed an MPC for EV aggregators, at which the EV aggregator receives payment through participation in frequency regulation market taking into account the users' convenience.					
[4]	Hierarchical	Yes	MILP	Yes	Real-time	Frequency-aware
	This paper presented a power management scheme for SFR using EVS. It proposed a 2-level hierarchical control mechanism which is validated based on real-time data acquired from PJM and CAISO.					
[7]	Distributed	Yes	MILP	Yes	Real-time	Economic-aware
	This paper developed an EV charging/discharging optimization algorithm that considers the prices of frequency regulation and electricity in the objective function. These prices are based on real and forecasting models.					
[9]	Distributed	Yes	NLP	Yes	Day-ahead and Real-time	Economic-aware
	This paper introduced an optimal bidirectional V2G process using a fleet of EVs connected to a distributed power system. The proposed system can reduce EV charging cost through participating in frequency and voltage regulation services.					
[17]	centralized	Yes	Stochastic MILP	No	Day-ahead	Economic-aware
	This paper investigated the participation of an aggregator controlling a fleet of EVs and an energy storage in day-ahead regulation and energy markets. Accordingly, the optimal size of the aggregator's bids is determined.					
[18]	centralized	No	Interior point method	Yes	Real-time	Frequency-aware
	This paper presented an aggregator-based hierarchical control mechanism for SFR using a fleet of EVs, at which EVs' scheduling optimization was formulated to provide optimum SFR, while satisfying EVs' energy demands.					
[19]	centralized	Yes	Gurobi	No	Real-time and Day-ahead	Frequency-aware
	This paper proposed game theoretic approaches using non-cooperative and cooperative game to leverage the use of EVs to provide frequency regulation services for the power grid.					
Proposed	Hierarchical	Yes	Pattern search	Yes	Day-ahead	Frequency-aware
	This paper presents a comparative study of the system performance at two different control layers. Thus, the minimum frequency imbalance is achieved, while considering the EV owners' preferences.					

pared an existing MILP-based scheme [4] to show the effectiveness of providing frequency regulation.
- The two models are compared under contingency cases.

2. System overview

The proposed control scheme evaluates the effectiveness of using EVs for frequency regulation on two different manners, as shown in Fig. 1(a) and (b), respectively. This control scheme was originally introduced in [4], at which the control units was located at the CS level. The proposed V2G system with bidirectional power flow consists of physical entities such as substation unit (SU), aggregators (AGs), and charging stations (CSs). Furthermore, frequency regulation capacity (FRC) estimators and multi-objective optimizer constitute the control layer of the proposed framework. First, the regulation signal is estimated and optimally dispatched among AGs and CSs. Then the optimum charging and discharging schedules for EVs are determined.

It can be noted that the charging/discharging behaviors of a set of EVs under each CS are defined when the original system is applied, referring Case 2, while the charging/discharging performance of each EV is separately controlled under the proposed framework, referring Case 1. Finally, minimum frequency fluctuations are, therefore, achieved.

Besides minimum frequency deviations, minimum battery degradation and maximum EV's profits are simultaneously obtained.

As proved in the literature, the battery's lifetime is highly affected by the frequent charging and discharging of the EV. The lithium-ion (Li-ion) batteries lifetime is considerably extended when its SoC is adjusted between 30 % – 50 %. On the contrary, maintaining the SoC between 70 % – 90 % or 20 % – 40 % yields a faster battery degradation according to the National Renewable Energy Laboratory (NREL) [25]. Therefore, the SoC of the EV batteries are adjusted between 30 % – 90 % through the overall process to minimize the battery degradation, while providing enhanced FRCs.

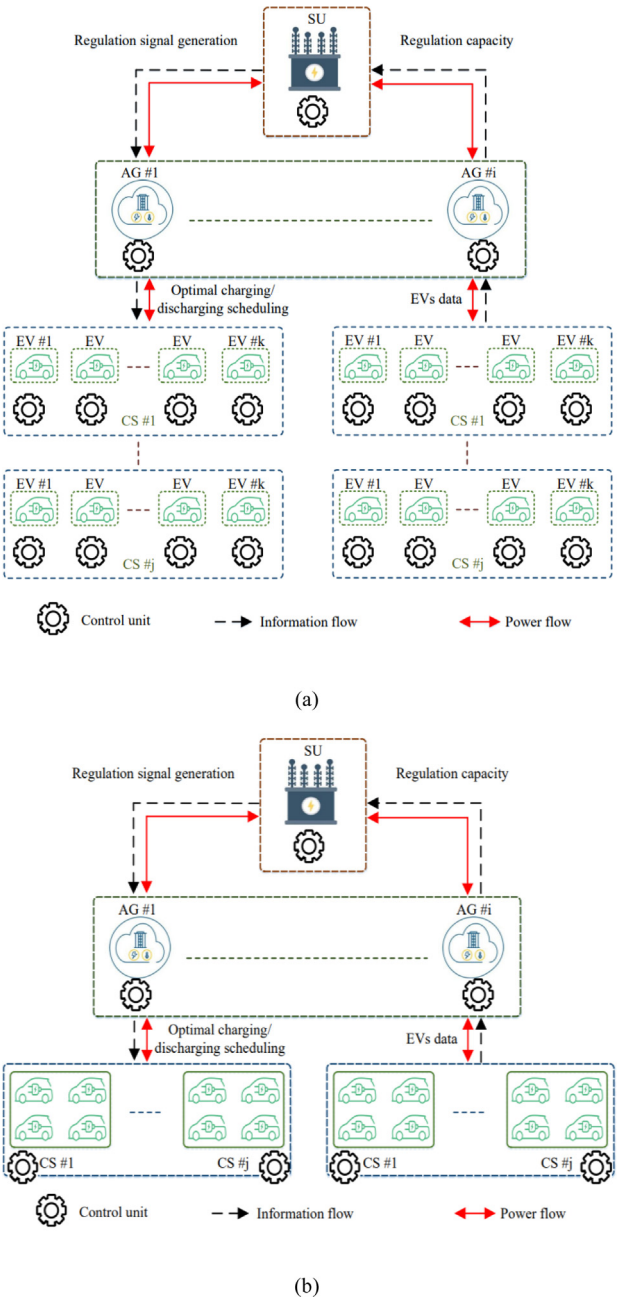

Fig. 1 Proposed V2G system framework. (a) Case 1. (b) Case 2.

Moreover, communication links between physical entities are provided to underpin real-time information flow. For instance, the SU monitors the frequency deviations and broadcasts regulation signal and regulation prices at time T. Meanwhile, regulation capacities at the AGs and CSs are computed by FRC estimators. The EVs' data, i.e., battery SoC, desired arrival and departure time, and vehicle charging requirements, are segregated to the AGs. Eventually, a multi-objective optimizer at the SU generates the optimum charging/discharging scheduling across the time intervals to track the regulation signal.

The communication network imposes different requirements including network coverage, throughput, latency, number of nodes and security [26]. The main communication technologies in the SG are GPRS-3G-LTE, WiMAX, WIFI, ZigBee, and power line communication (PLC) [27]. Amongst the communication technologies, PLC provides an easy way to install two-way communication infrastructure. Moreover, it can be effectively used for control, authentication, and payment of electric car charge. Moreover, PLC decrease failure risks by offering independent and redundant communication link [28].

3. Multi-objective optimization model

From a SG perspective, the frequency deviations, V2G support, optimal dispatch of the reference signal, and revenues of EVs are amongst the optimization objectives. It is worth mentioning that the afore-mentioned optimization objectives cannot be achieved simultaneously. Thus, the optimization model to achieve the optimum trade-off between these goals is proposed in both cases. An operating point that satisfies the operational constraints while being optimum with respect to the five objectives is, therefore, determined.

In this paper, the objective function (1) is minimized according to several decision variables x_i such as schedule charging and discharging rates at the EV level, i.e., $C_{ijk}^{sch}(\mathrm{T})$ and $D_{ijk}^{sch}(\mathrm{T})$, respectively. The provided set of equations mainly denotes the control scheme at the EV layer. Simple modification is needed to experiment the control at the CS layer such that the charging and discharging rates are equal at the CS level, i.e., $C_{ij}^{sch}(\mathrm{T})$ and $D_{ij}^{sch}(\mathrm{T})$, respectively. Precisely, the EVs located at a CS have the same $C_{ijk}^{sch}(\mathrm{T})$ and $D_{ijk}^{sch}(\mathrm{T})$. Moreover, several equality and inequality constraints are considered including FRCs of EVs, limitations on EV's battery SoC, and dispatch of reference signal between the CSs and AGs. FRCs of EVs are utilized to track the reference signal $\mathscr{R}^{ref}(\mathrm{T})$ at time intervals T. The EV battery SoC is maintained at specific limits to minimize the battery degradation. Furthermore, the design variables have lower and upper bounds (x_i^{min} and x_i^{max}). The objective function seeks to minimize the above-mentioned objectives considering the permissible EV charging and discharging capacities, and can be described as follows:

$$\min_{x_i} F(x_i) = \lambda_1 \frac{F_1(x_i)}{F_1'} + \lambda_2 \frac{F_2'}{F_2(x_i)} + \lambda_3 \frac{F_3'}{F_3(x_i)} + \lambda_4 \frac{F_4(x_i)}{F_4'} + \lambda_5 \frac{F_5'}{F_5(x_i)} \tag{1}$$

Where.

$$F_1(x_i) = \mathscr{R}^{ref}(\mathrm{T}) + \mathscr{P}_i^{down}(\mathrm{T}) - \mathscr{P}_i^{up}(\mathrm{T}) \tag{2}$$

$$F_2(x_i) = \mathscr{P}_i^{down}(\mathrm{T}) \tag{3}$$

$$F_3(x_i) = \mathscr{P}_i^{up}(\mathrm{T}) \tag{4}$$

$$F_4(x_i) = \mathscr{R}^{ref}(\mathrm{T}) - \sum_{i\in\mathrm{M}} \sum_{j\in\mathrm{N}} \left\{ \mathscr{R}_{11}^{ref}(\mathrm{T}) + \cdots + \mathscr{R}_{ij}^{ref}(\mathrm{T}) \right\} \tag{5}$$

$$F_5(x_i) = \sum_{i\in\mathrm{M}} \sum_{j\in\mathrm{N}} \times \sum_{k\in\mathrm{K}} \left\{ \left(\mathscr{P}_{ijk}^{down}(\mathrm{T}) * \mathscr{C}^{down}(\mathrm{T}) \right) + \left(\mathscr{P}_{ijk}^{up}(\mathrm{T}) * \mathscr{C}^{up}(\mathrm{T}) \right) \right\} \tag{6}$$

$$\overrightarrow{x_i} = \left[C_{ijk}^{sch}(\mathrm{T}), D_{ijk}^{sch}(\mathrm{T})\right]$$

where $F_1(x_i)$, $F_2(x_i)$, $F_3(x_i)$, $F_4(x_i)$, and $F_5(x_i)$ are the minimum frequency deviation, maximum charging V2G support, maximum discharging V2G support, optimal dispatch of reference signal, and maximum EVs profits, respectively. Meanwhile, the corresponding initial values are F_1', F_2', F_3', F_4', and F_5', respectively. Moreover, λ_1, λ_2, λ_3, λ_4, and λ_5 are the weight coefficients of the five objective functions, respectively, whereas $\lambda_1 + \lambda_2 + \lambda_3 + \lambda_4 + \lambda_5 = 1$.The frequency regulation is constrained by the following battery limits, optimal dispatch of reference signal among AGs and CSs, and total FRC constraints, as follows:

$$\mathscr{P}_{ijk}^{up}(\mathrm{T}) = \left(SoC_{ijk}^{ini}(\mathrm{T}) - SoC_{min}\right) * \frac{E_{ijk}^{rated} * D_{ijk}^{sch}(\mathrm{T})}{100} \tag{7}$$

$$\mathscr{P}_{ijk}^{down}(\mathrm{T}) = \left(SoC_{max} - SoC_{ijk}^{ini}(\mathrm{T})\right) * \frac{E_{ijk}^{rated} * C_{ijk}^{sch}(\mathrm{T})}{100} \tag{8}$$

$$\mathscr{P}_{ij}^{up}(\mathrm{T}) = \sum_{j\in\mathrm{N}} \sum_{k\in\mathrm{K}} \mathscr{P}_{ijk}^{up}(\mathrm{T}) \tag{9}$$

$$\mathscr{P}_{ij}^{down}(\mathrm{T}) = \sum_{j\in\mathrm{N}} \sum_{k\in\mathrm{K}} \mathscr{P}_{ijk}^{down}(\mathrm{T}) \tag{10}$$

$$\mathscr{P}_{i}^{up}(\mathrm{T}) = \sum_{i\in\mathrm{M}} \sum_{j\in\mathrm{N}} \sum_{k\in\mathrm{K}} \mathscr{P}_{ijk}^{up}(\mathrm{T}) \tag{11}$$

$$\mathscr{P}_{i}^{down}(\mathrm{T}) = \sum_{i\in\mathrm{M}} \sum_{j\in\mathrm{N}} \sum_{k\in\mathrm{K}} \mathscr{P}_{ijk}^{down}(\mathrm{T}) \tag{12}$$

$$\mathscr{P}^{tot}(\mathrm{T}) = \mathscr{P}_{i}^{up}(\mathrm{T}) + \mathscr{P}_{i}^{down}(\mathrm{T}) \tag{13}$$

Moreover, the reference regulation signal is optimally dispatched amongst the AGs and the CSs, as follows:

$$\mathscr{R}_{ij}^{ref}(\mathrm{T}) = \begin{cases} \mathscr{R}^{ref}(\mathrm{T}) \times \frac{\mathscr{P}_{ij}^{up}(\mathrm{T})}{\sum_{i\in\mathrm{M}}\sum_{j\in\mathrm{N}}\mathscr{P}_{ij}^{up}(\mathrm{T})}; for + ve \mathscr{R}^{ref}(\mathrm{T}) \\ \mathscr{R}^{ref}(\mathrm{T}) \times \frac{\mathscr{P}_{ij}^{down}(\mathrm{T})}{\sum_{i\in\mathrm{M}}\sum_{j\in\mathrm{N}}\mathscr{P}_{ij}^{down}(\mathrm{T})}; for - ve \mathscr{R}^{ref}(\mathrm{T}) \end{cases} \tag{14}$$

$$\mathscr{R}_{i}^{ref}(\mathrm{T}) = \sum_{j\in\mathrm{N}} \mathscr{R}_{ij}^{ref}(\mathrm{T}) \tag{15}$$

Finally, the average SoC of the batteries is maintained within the specified limits to minimize battery degradation. The lower and upper boundaries are considered as well.

$$SoC_{min} < SoC_{ijk}^{fin}(\mathrm{T}) < SoC_{max} \tag{16}$$

$$C_{min} < C_{ijk}^{sch}(\mathrm{T}) < C_{max} \tag{17}$$

$$D_{min} < D_{ijk}^{sch}(\mathrm{T}) < D_{max} \tag{18}$$

The determination of the weighting factors is crucial to the optimization approach; however, there is no specific standard to define these factors [29]. Based on the proposed dispatching strategy, minimum frequency deviation is crucial to maintain the balance between the demand and supply in the smart grid. Therefore, the corresponding weight factor is the highest, i.e., $\lambda_1 = 0.4$, to prioritize the first objective function F_1. While the remaining objectives have the same priority. Thus, the weighting factors are considered equal ($\lambda_2 = \lambda_3 = \lambda_4 = \lambda_5 = 0.15$).

4. Experimental results

The system is validated based on DSP and control Hardware-in-the-Loop (CHiL) using OPAL-RT, as shown in Fig. 2. The OPAL-RT platform is operating on 4 cores based on Intel Core Xeon processor at 3 GHz and RAM 2 × 8 GB. The system controller is uploaded on a 150 MHz DSP labeled as (TMS320F28335ZJZA). To validate the proposed day-ahead model, several scenarios have been implemented in the OPAL-RT using simulation parameters revealed in Table II:

- Scenario A: the innovative control model is compared to the conventional one. In that case, the optimization problem, presented in Section III, is applied to both models taking into consideration similar constraints, upper and lower boundaries, and EVs data including the EV state, initial SoC, and arrival and departure schedules.
- Scenario B: to further validate the proposed model, a comparison with the previously presented MILP-based model is elaborated. Therefore, the same simulation parameters are used under healthy condition.

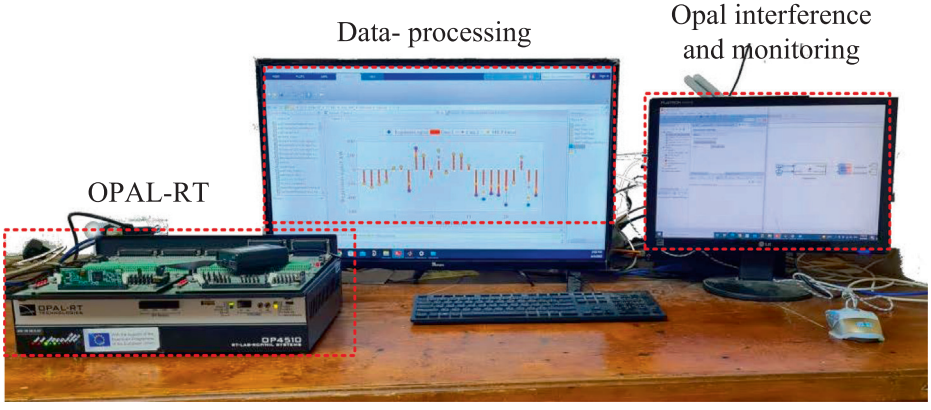

Fig. 2 Hardware-in-the-Loop system.

- Scenario C: both Case 1 and Case 2 are employed under contingency cases, a notable contribution of the presented study. In that case, the ability of the proposed model to trace the regulation signal under contingency cases is experimented.

4.1. Comparison of both cases under healthy conditions

This subsection compares the performance of the proposed control at the EV (Case 1) and CS (Case 2) layers in tracing the regulation signal on a day-ahead manner. The regulation signal is based on real-time traces obtained from PJM [4]. Fig. 3 shows how the two models approaching the regulation signal at almost all cases. For example, the regulation signal $\mathscr{R}^{ref}(t)$ is −360 kW at 24:00 and is met employing the proposed control model a the EV level, as shown in Fig. 3(a). On the other hand, the regulation signal is −500 kW at 20:00 and is met employing the control model at the CS level. Overall, the distributed model offers a lower minimum frequency fluctuation $F_1(x_i)$ of 963 kW compared to 1138 kW obtained from the centralized model. Fig. 3(b) depicts the grid frequency with respect to the presented models. The grid frequency is described based on the frequency droop characteristic and the droop gain given in [30]. Besides, the same number of EVs is used for charging and discharging, while their SoC is maintained within the optimal range, i.e., 30 % to 90 %, as depicted in Fig. 3(c) and (d), respectively. Accordingly, the battery degradation is minimized. At 24:00, the number of EVs for charging and discharging are 306 and 54, respectively.

Besides minimizing the grid frequency deviations, the proposed control scheme optimally dispatches the regulation signal among the AGs and CSs according to the estimated FRC of the AGs.

The performance results obtained in both cases are presented in Fig 0.4. the FRC for regulation up and down, i.e., $\mathscr{P}_i^{up}(t)$ and $\mathscr{P}_i^{down}(t)$, are shown in Fig. 4(a) and (b), respectively. For instance, $\mathscr{P}_i^{up}(t)$ is −85 kW and $\mathscr{P}_i^{up}(t)$ is 445 kW at 24:00 under the proposed control scheme at the EV layer. Whilst $\mathscr{P}_i^{up}(t)$ is −40 kW and $\mathscr{P}_i^{up}(t)$ is 174 kW at 24:00 under the control model at the CS layer. The optimal dispatch of the regulation signal among the AGs using both models is highlighted in Fig. 4(c) and (d). In Case 1, the scheduled reference signals for the AGs are −117, −124, and −115 kW, respectively. While −50, −34, and −50 kW constitute the scheduled reference signals at the AGs, respectively, in Case 2. The segregation of the reference signal among the CSs under both modes is shown in Fig. 4 (e) and (f). Furthermore, the scheduled charging and discharging rates, i.e., $C_{ijk}^{sch}(t)$ and $C_{ijk}^{sch}(t)$, are optimized, as explained in Section III. Under both modes, the values of $C_{ijk}^{sch}(t)$ and $C_{ijk}^{sch}(t)$ are obtained according to the limits revealed in Table II. In Case 1, the EV is directly controlled. Whereas a set of EVs at a CS are controlled by the AG in Case2. As an illustrative example, the scheduled charging and discharging rates of four CSs are shown in Fig. 4 (h) and (i), respectively, at the CS level.

Finally, maximum profits of EVs participating in frequency regulation are considered. The regulation prices, i.e., $\mathscr{C}^{up}(t)$ and $\mathscr{C}^{up}(t)$, are acquired from CAISO [4], as depicted in Fig. 5(a). The $\mathscr{C}^{up}(t)$ and $\mathscr{C}^{down}(t)$ are 6.2 and 3.5 $ at 24:00 in both modes, respectively. The analysis of the cumulative EV's revenues shows that the profits are higher in Case 1when

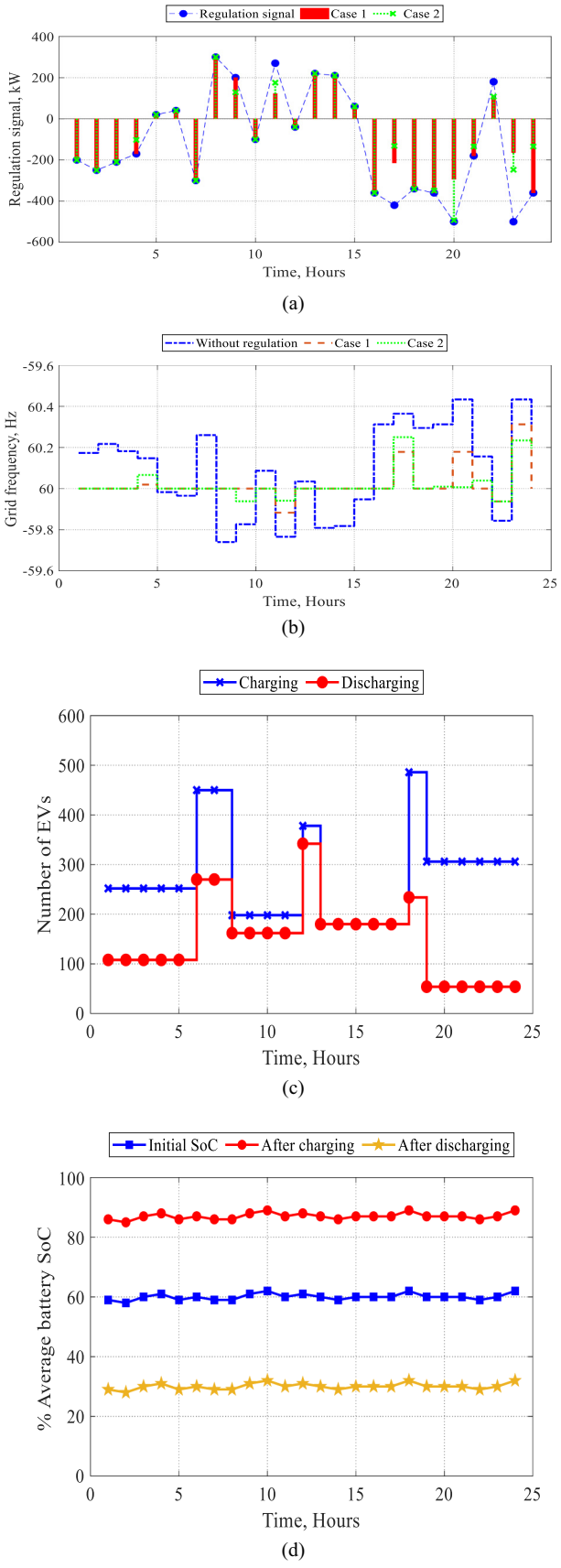

Fig. 3 Comparison of control schemes at the CS level (Case 1) and at the EV level (Case 2). (a) Frequency regulation support. (b) Grid frequency. (c) Number of EVs. (d) Average battery SoC.

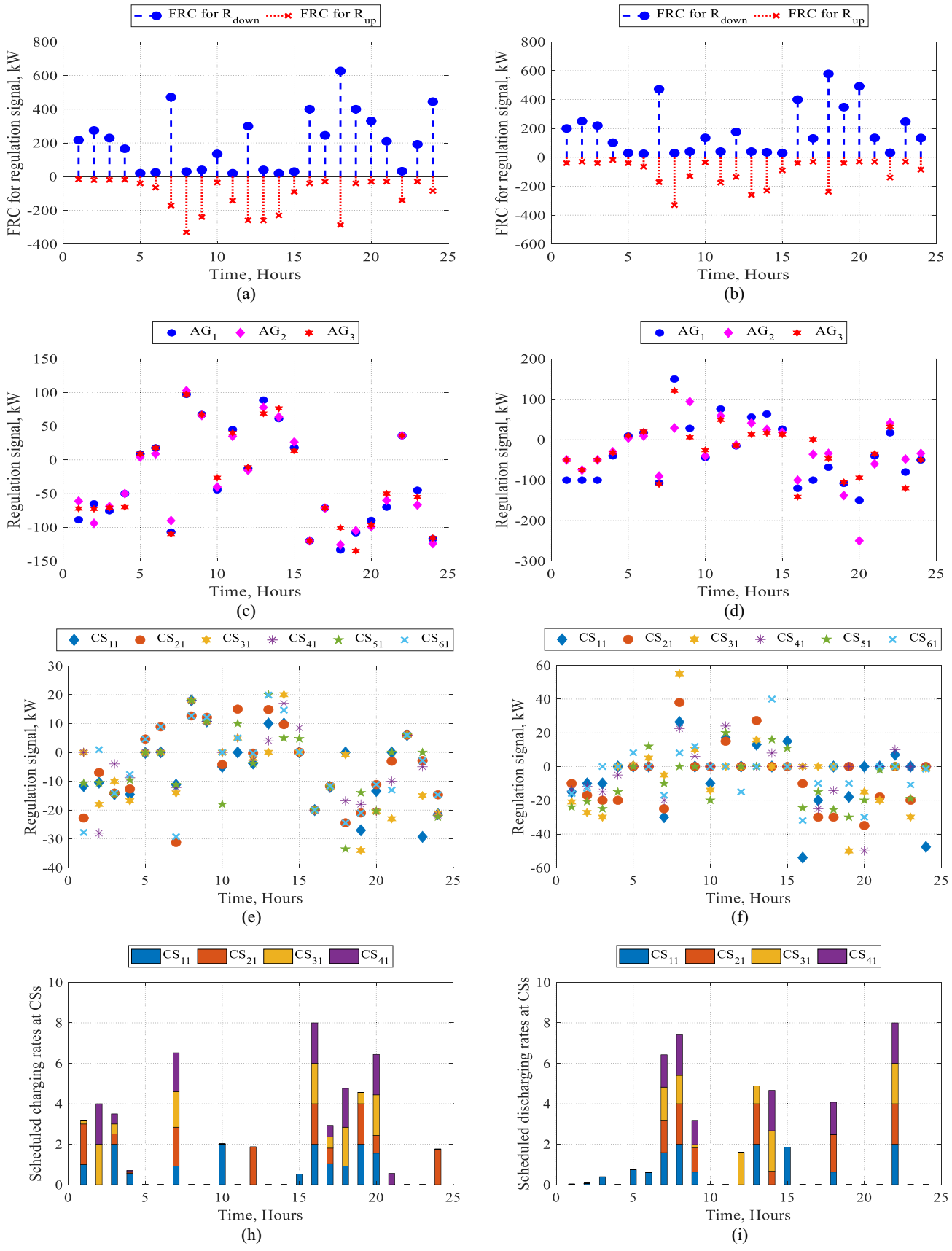

Fig. 4 Simulation resulted obtained under both distributed and centralized modes. (a) FRC (Case 1). (b) FRC (Case 2). (c) regulation signal dispatch among AGs (Case 1). (d) regulation signal dispatch among AGs (Case 2). (e) regulation signal dispatch among CSs (Case 1). (f) regulation signal dispatch among CSs (Case 2). (h) Scheduled charging rates (Case 2). (i) Scheduled discharging rates (Case 2).

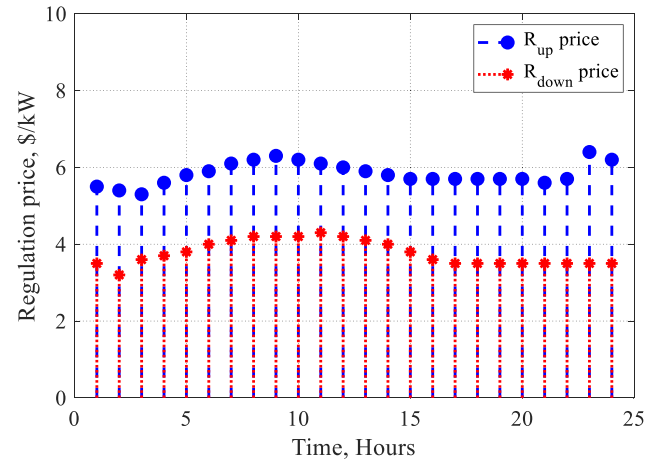

(a)

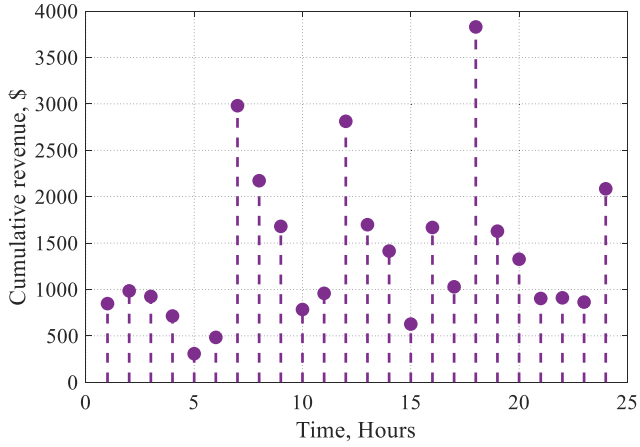

(b)

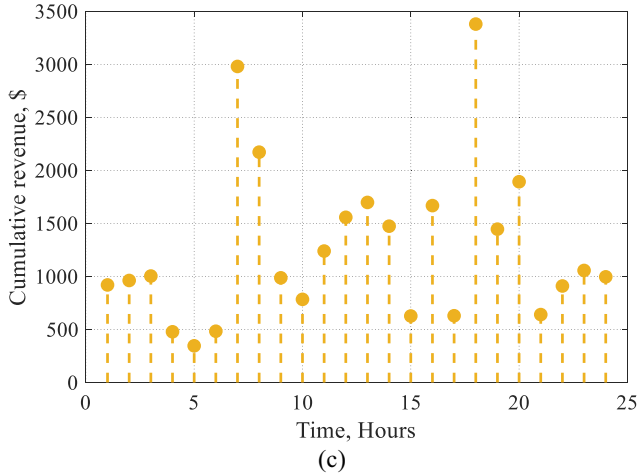

(c)

Fig. 5 EV revenues. (a) regulation prices from CAISO for the year 2014. (b) Cumulative revenues (Case 1). (c) Cumulative revenues (Case 2).

compared to Case 2, as shown in Fig. 5(b) and (c), respectively. For example, at 24:00 the cumulative daily profits earned by the employed EVs are 2085 $ and 996.4 $ when the control is applied at the EVs and CSs, respectively.

Table 2 Simulation parameters.

Parameter	Value	Parameter	Value
No. of AGs	3	Minimum SoC (%)	30
No. of CSs	6	Maximum SoC (%)	90
No. of EVs/CS	80	C_{min}/D_{min}	0
EV energy (kWh)	16	C_{max}/D_{max}	2
Average SoC (%)	60		

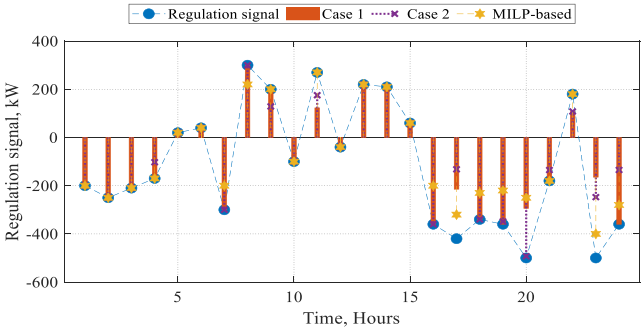

Fig. 6 Frequency regulation support using the proposed schemes and the MILP-based one.

Table 3 Quantitative analysis of the percentage of the regulation signal met by under health conditions.

	Case 1	Case 2	MILP
Healthy case	83.37 %	80.34 %	80.72 %

4.2. Comparison with a MILP-based one

To further verify the efficacy of the proposed models, they are compared to an existing control scheme [4]. The existing scheme is a 2-level hierarchical control based on MILP optimization to minimize the frequency deviation. It can be noted that the EVs charging and discharging rated are kept constant at the CSs. For fair comparison, the same simulation parameters are used, as listed in Table 2. The proposed control schemes as well as the MILP-based one meet the regulation signal at majority of time slots, as presented in Fig. 6.

Moreover, a quantitative analysis of the percentage of the regulation signal met is provided to assess the system performance when different control schemes are employed, as revealed in Table 3. The proportion of the regulation signal met is given by (19):

$$R_{met} = 100 - \frac{\sum |F_1(\mathrm{T})|}{\sum |\mathscr{R}^{ref}(\mathrm{T})|} * 100 \tag{19}$$

where $\sum |F_1(\mathrm{T})|$ is the absolute sum of the imbalance of the regulation signal and $\sum |\mathscr{R}^{ref}(\mathrm{T})|$ the power from the EVs and is the absolute sum of the regulation signal.

Although Case 2 and MILP-based models track the regulation signal in different manners, they offer almost the same percentage of the regulation signal met with 80.34 % and 80.72 %, respectively. On the other hand, the novel control

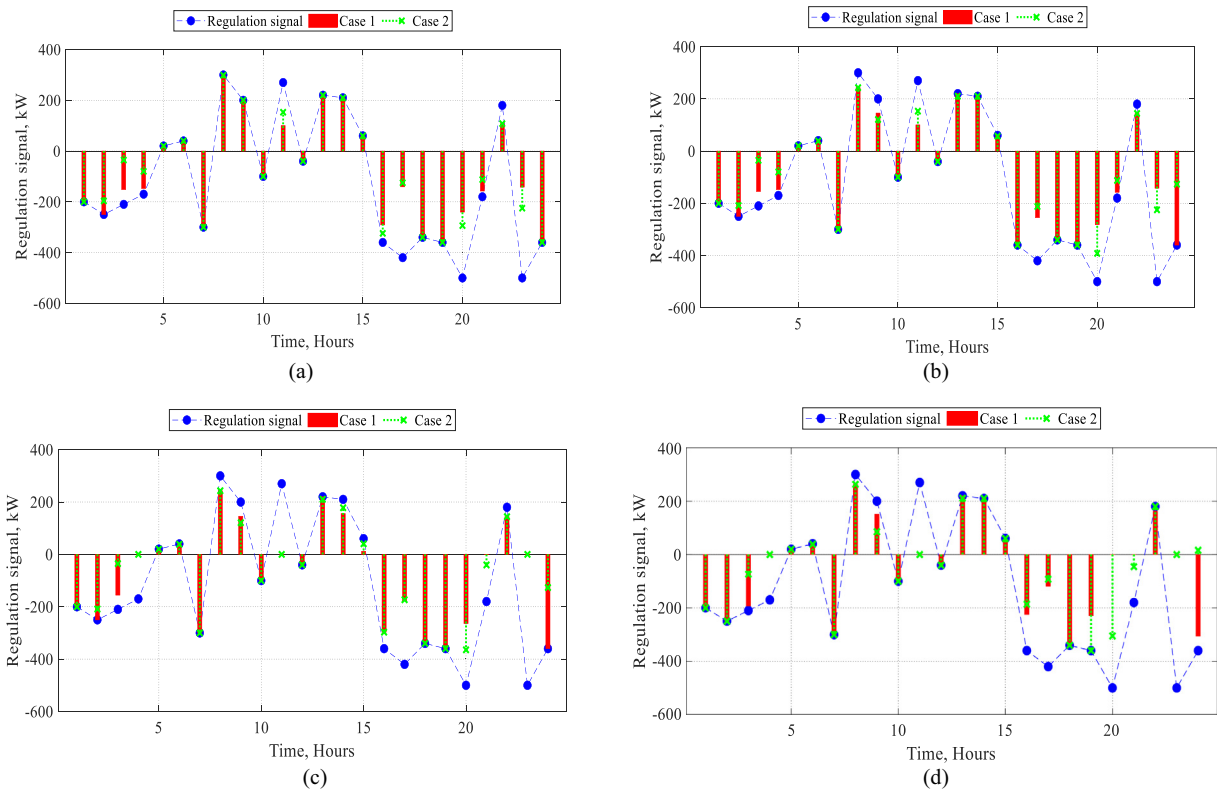

Fig. 7 Performance of the distributed and centralized models under contingency cases. (a) Contingency 1. (b) Contingency 2. (c) Contingency 3. (d) Contingency 4.

Table 4 Quantitative analysis of the percentage of the regulation signal met by under contingency conditions.

	Case 1	Case 2	Difference
Contingency 1	81.81 %	76.06 %	+5.75 %
Contingency 2	80.80 %	74.12 %	+6.68 %
Contingency 3	70.54 %	67.05 %	+3.50 %
Contingency 4	70.23 %	64.40 %	+5.83 %

scheme (Case 1) gives the best behavior since it yields an increase in the regulation signal met proportion by 3 % when compared to the other models.

4.3. Contingency cases

The impact of an EV charging station on the grid has been intensively presented in the literature [31–33]. It was concluded that distribution networks could withstand the penetration of EVs up to a certain level. Moreover, the voltage profile degradation is observed at the weak bus due to the escalating EV charging loads [32]. The unregulated charging and discharging behaviours of EVs not only yields contingencies at the CS level but also the loss of the CS itself. In this study, four contingency cases, namely Contingency 1 – 4, are simulated considering the loss of single CS (Contingency 1) up to the loss of four CSs (Contingency 4).

Fig. 7 shows the performance of both control schemes at the EVs and CSs under the above-mentioned contingencies. It is clear that the proposed control model at the EVs shows outstanding behaviour achieving the regulation signal up to the loss of two CSs. However, the performance of the centralized model is degraded. Despite the fact that the proposed model (Case 1) can hardly meet the regulation signal after the loss of more than two CSs, its performance is considerably better than the conventional one (Case 2). To further investigate the superiority of the novel distributed model, a quantitative analysis of the achieved regulation signal percentage by (19) is listed in Table 4. The proposed controller at the EV level can meet the regulation with 5.75 % and 6.68 % higher than the one at the CS level in Contingencies 1 and 2, respectively. However, the performance of both control schemes degrades after the loss of two CSs; namely, Contingency 2. As a result, the ability of the proposed model to meet the regulation signal under both healthy and contingency condition is proved.

5. Conclusions

This paper proposes a novel power control scheme for secondary frequency regulation using EVs integrated within the power grid. In addition, a dispatching strategy is developed based on the available literature for the sake of comparison. In both models, the charging/discharging behaviours of EVs are optimized based on the pattern search multi-objective optimization approach. Simulations showed the effectiveness of both models in tracing the regulation signals while highlighting the superiority of the proposed model. Another notable contribution of the presented analysis is the comparison of both models under contingency cases. Accordingly, the ability of the proposed control scheme to achieve the minimum fre-

quency deviations, up to the loss of two CSs, is highlighted. Finally, the proposed model has shown outstanding performance over an existing MILP-based model. In healthy case, the control scheme at the EV level can meet the regulation with 3.37 % higher than the control scheme at the CS level and the MILP-based model; however, at a heavy computational burden. Moreover, the controller in Case 1 can meet the regulation with 5.75 % and 6.68 % higher than the one in Case 2 in contingency 1 and 2, respectively. The following aspects are identified as the possible future research trends in this context [11]:

- Modified prediction model including real-time weather conditions and system load demand.
- Interaction between ancillary service providers and an EV aggregator in competitive markets.
- Integration of the lithium-ion battery ageing model into V2G operation.

Declaration of Competing Interest

The authors declare that they have no known competing financial interests or personal relationships that could have appeared to influence the work reported in this paper.

Acknowledgements

This work was achieved by the financial support of ITIDAs ITAC collaborative funded project under the category type of advanced research projects (ARP) and grant number ARP2020.R29.7.

References

[1] A. Ghasempour and J. Lou, "Advanced metering infrastructure in smart grid: Requirements challenges architectures technologies and optimizations," in *Smart Grids: Emerging Technologies, Challenges and Future Directions*: Nova Science Publishers Hauppauge, NY, USA, 2017, pp. 1-8.

[2] M. Wang, Y. Mu, Q. Shi, H. Jia, F. Li, Electric vehicle aggregator modeling and control for frequency regulation considering progressive state recovery, IEEE Transactions on Smart Grid 11 (5) (2020) 4176–4189.

[3] S. Cai and R. Matsuhashi, "Model Predictive Control for EV Aggregators Participating in System Frequency Regulation Market," *IEEE Access,* 2021.

[4] K. Kaur, N. Kumar, M. Singh, Coordinated power control of electric vehicles for grid frequency support: MILP-based hierarchical control design, IEEE transactions on smart grid 10 (3) (2019) 3364–3373.

[5] C. Xue, H. Zhou, Q. Wu, X. Wu, X. Xu, Impact of Incentive Policies and Other Socio-Economic Factors on Electric Vehicle Market Share: A Panel Data Analysis from the 20 Countries, Sustainability 13 (5) (2021) 2928.

[6] S. Zhang, K.-C. Leung, Joint optimal power flow routing and vehicle-to-grid scheduling: Theory and algorithms, IEEE Transactions on Intelligent Transportation Systems (2020).

[7] O. Kolawole, I. Al-Anbagi, Electric vehicles battery wear cost optimization for frequency regulation support, IEEE Access 7 (2019) 130388–130398.

[8] G. Xiao, C. Li, Z. Yu, Y. Cao, B. Fang, Review of the impact of electric vehicles participating in frequency regulation on power grid, in: 2013 ChInese automation congress, IEEE, 2013, pp. 75–80.

[9] S.-A. Amamra, J. Marco, Vehicle-to-grid aggregator to support power grid and reduce electric vehicle charging cost, IEEE Access 7 (2019) 178528–178538.

[10] C. Peng, J. Zou, L. Lian, Dispatching strategies of electric vehicles participating in frequency regulation on power grid: A review, Renewable Sustainable Energy Reviews 68 (2017) 147–152.

[11] M.Y. Metwly, M.S. Hamad, A.S. Abdel-Khalik, H. Eldesouki, A Review of Power Management Strategies for Grid Frequency Regulation Using Electric Vehicles, in: 2021 22nd International Middle East Power Systems Conference (MEPCON), IEEE, 2021, pp. 541–547.

[12] S. Han, S.J.E. Han, Economic feasibility of V2G frequency regulation in consideration of battery wear 6 (2) (2013) 748–765.

[13] E. Yao, V. W. Wong, and R. J. I. T. o. S. G. Schober, "Robust frequency regulation capacity scheduling algorithm for electric vehicles," vol. 8, no. 2, pp. 984-997, 2016.

[14] D. Liu, Cluster control for EVS participating in grid frequency regulation by using virtual synchronous machine with optimized parameters, Applied Sciences 9 (9) (2019) 1924.

[15] M. Latifi, R. Sabzehgar, P. Fajri, M. Rasouli, A Novel Control Strategy for the Frequency and Voltage Regulation of Distribution Grids Using Electric Vehicle Batteries, Energies 14 (5) (2021) 1435.

[16] N. Neofytou, K. Blazakis, Y. Katsigiannis, G. Stavrakakis, Modeling vehicles to grid as a source of distributed frequency regulation in isolated grids with significant RES penetration, Energies 12 (4) (2019) 720.

[17] B. Vatandoust, A. Ahmadian, M.A. Golkar, A. Elkamel, A. Almansoori, M. Ghaljehei, Risk-averse optimal bidding of electric vehicles and energy storage aggregator in day-ahead frequency regulation market, IEEE Transactions on Power systems 34 (3) (2018) 2036–2047.

[18] K. Kaur, M. Singh, N. Kumar, Multiobjective optimization for frequency support using electric vehicles: An aggregator-based hierarchical control mechanism, IEEE Systems Journal 13 (1) (2017) 771–782.

[19] X. Chen, K.-C. Leung, Non-cooperative and cooperative optimization of scheduling with vehicle-to-grid regulation services, IEEE Transactions on Vehicular Technology 69 (1) (2019) 114–130.

[20] M. Wang et al, State space model of aggregated electric vehicles for frequency regulation, IEEE Transactions on Smart Grid 11 (2) (2019) 981–994.

[21] R. Kumar, D. Saxena, Fault analysis of a distribution system embedded with plug-in electric vehicles, in: 2017 Recent Developments in Control, Automation & Power Engineering (RDCAPE), IEEE, 2017, pp. 230–234.

[22] S. Shojaabadi, S. Abapour, M. Abapour, A. Nahavandi, Optimal planning of plug-in hybrid electric vehicle charging station in distribution network considering demand response programs and uncertainties, IET Generation, Transmission & Distribution 10 (13) (2016) 3330–3340.

[23] S. Deb, K. Tammi, K. Kalita, P. Mahanta, Impact of electric vehicle charging station load on distribution network, Energies 11 (1) (2018) 178.

[24] B. Zhou, T. Littler, L. Meegahapola, Assessment of transient stability support for electric vehicle integration, in: 2016 IEEE Power and Energy Society General Meeting (PESGM), IEEE, 2016, pp. 1–5.

[25] J. Tan, Y. Zhang, Coordinated control strategy of a battery energy storage system to support a wind power plant providing multi-timescale frequency ancillary services, IEEE Transactions on Sustainable Energy 8 (3) (2017) 1140–1153.

[26] IEEE Guide for Smart Grid Interoperability of Energy Technology and Information Technology Operation with the Electric Power System (EPS), End-Use Applications, and Loads, 2011.

[27] E. Tsampasis, D. Bargiotas, C. Elias, and L. Sarakis, "Communication challenges in smart grid," in *MATEC web of conferences*, 2016, vol. 41, p. 01004: EDP Sciences.

[28] N. Navet, Y. Song, F. Simonot-Lion, and C. Wilwert, "Trends in automotive communication systems," *Proceedings of the IEEE,* vol. 93, no. 6, pp. 1204-1223, 2005.

[29] G. D. Yalcin and N. Erginel, "Determining weights in multi-objective linear programming under fuzziness," in *Proceedings of the World Congress on Engineering*, 2011, vol. 2, pp. 6-8.

[30] Z. Liu, J. Yang, Y. Zhang, T. Ji, J. Zhou, Z. Cai, Multi-objective coordinated planning of active-reactive power resources for decentralized droop-controlled islanded microgrids based on probabilistic load flow, IEEE Access 6 (2018) 40267–40280.

[31] J. de Hoog et al, The importance of spatial distribution when analysing the impact of electric vehicles on voltage stability in distribution networks, Energy Systems 6 (1) (2015) 63–84.

[32] M. Geske, P. Komarnicki, M. Stötzer, and Z. A. Styczynski, "Modeling and simulation of electric car penetration in the distribution power system—Case study," in *Modern Electric Power Systems*, 2010, pp. 1-6: IEEE.

[33] Y. Zhang, X. Song, F. Gao, J. Li, Research of voltage stability analysis method in distribution power system with plug-in electric vehicle, in: 2016 IEEE PES Asia-Pacific Power and Energy Engineering Conference (APPEEC), IEEE, 2016, pp. 1501–1507.